EUROPEAN ORGANIZATION FOR NUCLEAR RESEARCH

CERN-EP-2022-121
07 June 2022

Observation of flow angle and flow magnitude fluctuations in Pb–Pb collisions at $\sqrt{s_{\mathrm{NN}}}$ = 5.02 TeV at the LHC

ALICE Collaboration

Abstract

This Letter reports on the first measurements of transverse momentum dependent flow angle Ψ_n and flow magnitude v_n fluctuations, determined using new four-particle correlators. The measurements are performed for various centralities in Pb–Pb collisions at a centre-of-mass energy of $\sqrt{s_{\mathrm{NN}}}$ = 5.02 TeV with ALICE at the LHC. Both flow angle and flow magnitude fluctuations are observed in the presented centrality ranges and are strongest in the most central collisions and for a transverse momentum $p_{\mathrm{T}} > 2$ GeV/c. Comparison with theoretical models, including iEBE-VISHNU, MUSIC, and AMPT, show that the measurements bring novel insights into the fluctuating initial conditions that are not well known. In addition, these new results exhibit unique sensitivities to the specific shear viscosity, η/s, of the quark–gluon plasma (QGP) and to the initial state of the heavy-ion collisions. As such fluctuations are getting stronger with increasing p_{T}, a re-examination of existing models is needed to have a more precise and unbiased extraction of properties of the QGP.

In ultrarelativistic collisions of heavy ions, such as those at the Relativistic Heavy-Ion Collider (RHIC) and the Large Hadron Collider (LHC), a deconfined state of strongly interacting matter, commonly referred to as quark–gluon plasma (QGP), is predicted to be created under extreme conditions of temperature and energy densities [1, 2]. Many experimental results indicate that a strongly-coupled QGP is formed in heavy-ion collisions [3–7]. Initial anisotropies of the geometric overlap of the colliding nuclei and spatial inhomogeneities in the energy density drive the collective expansion of the QGP and are transformed through the evolution of the QGP into a momentum anisotropy in the final state [8–10]. This momentum anisotropy is characterised by a Fourier expansion of the distribution of the azimuthal angle, φ, of emitted particles [11]

$$\frac{\mathrm{d}^2N}{\mathrm{d}p_\mathrm{T}\mathrm{d}\varphi} = \frac{\mathrm{d}N}{2\pi\mathrm{d}p_\mathrm{T}}\left(1+2\sum_{n=1}^{\infty} v_n(p_\mathrm{T})\cos[n(\varphi-\Psi_n(p_\mathrm{T}))]\right), \tag{1}$$

where $v_n(p_\mathrm{T})$ and $\Psi_n(p_\mathrm{T})$ correspond to the magnitude and angle, respectively, of the n^{th}-order harmonic flow vector $\vec{V}_n(p_\mathrm{T}) = v_n(p_\mathrm{T})e^{in\Psi_n(p_\mathrm{T})}$. Here the transverse momentum, p_T, dependence of both the flow magnitude and flow angle has been made explicit. The flow vector quantifies the orientation and magnitude of the anisotropic flow, and the flow angle Ψ_n is the angle of the symmetry plane of the n^{th}-order flow vector.

Typically, the largest flow coefficient is the elliptic flow v_2, since it is largely determined by the geometrical overlap of nuclei colliding at a finite impact parameter, the distance between the nuclei centres in the transverse plane. However, fluctuations in the position of the colliding nuclei and in the position of nucleons within the nuclei can induce more complex geometrical shapes, which will give rise to non-zero flow coefficients with $n > 2$ [12–15], such as the triangular flow v_3. Both elliptic and triangular flow coefficients have been measured extensively at RHIC [16–19] and at the LHC [20–30]. The comparison of measurements of v_n at low p_T with hydrodynamical calculations has been used to constrain the initial conditions of the heavy-ion collisions and the transport properties of the QGP, such as the specific shear viscosity η/s. These comparisons indicate that the system behaves as a strongly-coupled low-viscosity fluid [10, 31–33]. Studies probing the collective expansion of the system using hard probes, such as measurements of the anisotropic flow of charged and identified hadrons at high p_T [34–39], or of hadrons containing heavy quarks [40–52], rely on the comparison of theoretical model calculations to experimental data to extract the QGP properties, such as the path-length dependence of the heavy-quark energy loss [53, 54]. In this Letter, the observation of separate flow angle and flow magnitude fluctuations in heavy-ion data is presented. It is argued that the notion of a common symmetry plane, widely used in various flow measurements, does not hold in measurements that correlate particles at high p_T (> 2 GeV) with the common symmetry plane determined mainly by low p_T particles.

Fluctuations of both the flow angle Ψ_n and the flow magnitude v_n have been shown to be present in hydrodynamical models [55, 56]. The flow angle fluctuations are the fluctuations of the symmetry plane determined by a subset of the particles, in this case, those at a specific p_T, with respect to the symmetry plane determined by the total set of particles. In heavy-ion collisions, the produced particle yield is typically dominated by low p_T particles. The flow magnitude fluctuations can be understood as the fluctuations of the v_n coefficients at different transverse momentum ranges. Measurements at the LHC have reported the existence of p_T-dependent flow vector fluctuations [57–60]. However, those measurements rely on observables constructed from two-particle correlations, which intrinsically contain contributions from both the flow angle and magnitude fluctuations with no way to separate the two experimentally. A Principal Component Analysis (PCA) has been used for the extraction of leading and subleading modes of flow fluctuations in heavy-ion collisions [61–64]. However, these analyses were also based on information retrieved from two-particle correlations and cannot be used to separate the individual components of the flow vector fluctuations. In this Letter, we propose new four-particle correlation functions to separate the p_T-dependent fluctuations of the flow angle and flow magnitude. The flow angle fluctuations can be quantified by

$$A_n^{\mathrm{f}} = \frac{\langle\langle \cos n[\varphi_1^{\mathrm{a}} + \varphi_2^{\mathrm{a}} - \varphi_3 - \varphi_4]\rangle\rangle}{\langle\langle \cos n[\varphi_1^{\mathrm{a}} + \varphi_2 - \varphi_3^{\mathrm{a}} - \varphi_4]\rangle\rangle} = \frac{\langle v_n^2(p_{\mathrm{T}}^{\mathrm{a}})\, v_n^2 \cos 2n[\Psi_n(p_{\mathrm{T}}^{\mathrm{a}}) - \Psi_n]\rangle}{\langle v_n^2(p_{\mathrm{T}}^{\mathrm{a}}) v_n^2\rangle} \simeq \langle \cos 2n\,[\Psi_n(p_{\mathrm{T}}^{\mathrm{a}}) - \Psi_n]\rangle_{\mathrm{w}}, \quad (2)$$

where the a superscript refers to an *associate* particle selected from a narrow transverse momentum range $p_{\mathrm{T}}^{\mathrm{a}}$ and the w means that A_n^{f} is averaged over the event ensemble with each event having a weight of the fourth power of v_n [65]. The double brackets refer to an average over all particles and all events, and the single brackets refer to an average over all events. A value of $A_n^{\mathrm{f}} < 1$ indicates the presence of p_{T}-dependent flow angle fluctuations. A larger deviation from unity suggests that the symmetry plane at a specific p_{T} is more decorrelated with respect to the common symmetry plane. On the other hand, the flow magnitude fluctuations can be studied with the double ratio

$$M_n^{\mathrm{f}} = \frac{\langle\langle \cos n[\varphi_1^{\mathrm{a}} + \varphi_2 - \varphi_3^{\mathrm{a}} - \varphi_4]\rangle\rangle / \left(\langle\langle \cos n[\varphi_1^{\mathrm{a}} - \varphi_3^{\mathrm{a}}]\rangle\rangle \langle\langle \cos n[\varphi_2 - \varphi_4]\rangle\rangle\right)}{\langle\langle \cos n[\varphi_1 + \varphi_2 - \varphi_3 - \varphi_4]\rangle\rangle / \langle\langle \cos n[\varphi_1 - \varphi_2]\rangle\rangle^2} = \frac{\langle v_n^2(p_{\mathrm{T}}^{\mathrm{a}}) v_n^2\rangle / \langle v_n^2(p_{\mathrm{T}}^{\mathrm{a}})\rangle \langle v_n^2\rangle}{\langle v_n^4\rangle / \langle v_n^2\rangle^2}. \quad (3)$$

A deviation of M_n^{f} from unity indicates the presence of p_{T}-dependent flow magnitude fluctuations. The magnitude of the deviation will show how strongly the flow magnitude is decorrelated at a specific p_{T} range with respect to the integrated flow. These new correlators probe a higher moment of the distribution of flow fluctuations compared to correlators traditionally used in studies of flow and flow fluctuations using two-particle techniques [57–59]. The lower-order moments of the flow angle and flow magnitude fluctuations cannot be measured separately in experiments but can be approximated by constructing the lower and upper limits of the first moment of flow angle and magnitude fluctuations, respectively. The lower limit of the first-moment flow angle fluctuations $\langle \cos n\,[\Psi_n(p_{\mathrm{T}}^{\mathrm{a}}) - \Psi_n]\rangle$ can be calculated as

$$\sqrt{\frac{A_n^{\mathrm{f}} + 1}{2}} \geq \langle \cos n[\Psi_n(p_{\mathrm{T}}^{\mathrm{a}}) - \Psi_n]\rangle. \quad (4)$$

The overall flow vector fluctuations can be probed by the ratio of the p_{T}-differential flow coefficient $v_n\{2\} = \langle v_n(p_{\mathrm{T}}^{\mathrm{a}}) v_n \cos n[\Psi_n(p_{\mathrm{T}}^{\mathrm{a}}) - \Psi_n]\rangle / \sqrt{\langle v_n^2\rangle}$ and the p_{T}-integrated flow coefficient in a narrow p_{T} interval $v_n[2] = \sqrt{\langle v_n^2(p_{\mathrm{T}}^{\mathrm{a}})\rangle}$ [55]. Taking the ratio of Eq. (4) and the flow vector fluctuations

$$v_n\{2\}/v_n[2] = \frac{\langle v_n(p_{\mathrm{T}}^{\mathrm{a}})\, v_n \cos n\,[\Psi_n(p_{\mathrm{T}}^{\mathrm{a}}) - \Psi_n]\rangle}{\sqrt{\langle v_n^2(p_{\mathrm{T}}^{\mathrm{a}})\rangle}\sqrt{\langle v_n^2\rangle}}, \quad (5)$$

enables the calculation of the upper limit of the first-order flow magnitude fluctuations

$$\frac{v_n\{2\}/v_n[2]}{\sqrt{(A_n^{\mathrm{f}} + 1)/2}} \leq \frac{\langle v_n(p_{\mathrm{T}}^{\mathrm{a}})\, v_n\rangle}{\sqrt{\langle v_n^2(p_{\mathrm{T}}^{\mathrm{a}})\rangle}\sqrt{\langle v_n^2\rangle}}. \quad (6)$$

The limits on the first-moment flow angle and magnitude fluctuations connect the study of the separated fluctuations with the previous studies of flow vector fluctuations using only two-particle correlations [57–59]. All the above correlators are calculated with the generic framework [66, 67], which corrects the non-uniformities in the acceptance of the detector. As the correlations in Eqs. (2) and (3) are themselves correlated, the statistical uncertainty is estimated by the bootstrap method of random sampling with replacement.

The correlators A_2^{f} and M_2^{f} are measured in approximately 54 million Pb–Pb collisions collected in 2015 at a centre-of-mass energy per nucleon pair of $\sqrt{s_{\mathrm{NN}}}$ = 5.02 TeV. Experimentally, events are selected based on a minimum bias trigger achieved by requiring a coincidence of signals in the two V0 scintillator arrays, V0A with a pseudorapidity range $2.8 < \eta < 5.1$, and V0C with a pesudorapidity range

$-3.7 < \eta < -1.7$. Additionally, a reconstructed primary vertex within ± 10 cm of the nominal interaction point along the beam axis is required. Rejection of pileup events, which are events close in time to the triggered event due to the high luminosity, is based on the correlation between tracks measured with different detectors. A variation of the criteria for pileup rejection is considered for the systematic uncertainties [68]. The centrality of the events is measured using a fit of the V0A and V0C signal amplitude sum, with a two-component model for particle production and a Glauber Monte Carlo model of the collision geometry [69]. Charged tracks are reconstructed using the Inner Tracking System (ITS) [70] and the Time Projection Chamber (TPC) [71]. Tracks are selected with at least 70 TPC space points out of 159 points, and a χ^2 per TPC cluster less than 4 [72]. To reduce contamination from secondary particles, tracks are selected with a distance of closest approach to the primary vertex of less than 2 cm in the longitudinal direction and a p_{T}-dependent selection ranging from 0.2 cm at p_{T} = 0.2 GeV/c to 0.018 cm at p_{T} = 4.0 GeV/c in the transverse direction. Additionally, charged particle tracks are selected within the kinematic range $|\eta| < 0.8$ and $0.2 < p_{\mathrm{T}} < 5$ GeV/c. In order to suppress non-flow correlation contributions, which are not related to collective behaviour, such as resonance decays and jets, a gap in pseudorapidity is introduced between the correlated particles. An η-gap of $|\Delta\eta| > 0.8$ is used for two-particle correlations and $|\Delta\eta| > 0$ for four-particle correlations in order to ensure optimal balance between the statistical precision and non-flow suppression. To further investigate the non-flow suppression, the analysis was also performed with only particles of same-sign charge and with increasing pseudorapidity gaps between the subevents of correlated particles. Additional Monte Carlo studies using HIJING [73], a model that does not feature collective effects, but involves particle correlations arising from other sources, indicate that non-flow is sufficiently suppressed with the applied pseudorapidity gaps. Based on these model studies, the non-flow correlation contributions to the correlators are less than 1% of the measured value across the presented centralities.

Systematic uncertainties are evaluated by varying the event and track selection criteria. Since the systematic uncertainty may depend on the collision centrality and the p_{T} of particles, only the largest contribution from each source is mentioned below. The systematic uncertainty associated to the event selection criteria is evaluated by varying the selection on the vertex position along the beam direction (from 10 cm to 7, 8, or 9 cm), the magnetic field polarity, and the criteria for selecting pileup events, and is below 1%. Possible biases from the centrality determination were investigated by repeating the analysis using the centrality estimated at midrapidity from hits in the Silicon Pixel Detector (SPD) instead of the V0, resulting in a negligible difference. Uncertainties related to track selection are estimated by considering different track reconstruction and track quality selection criteria. Changing the track reconstruction to include tracks without hits in the SPD leads to a variation of at most 1.7%. The quality of the reconstructed tracks is varied by changing the minimum number of TPC space points to 80 and 90, which leads to a difference of 1.5% on the measured correlators. Uncertainties related to the variations in the distance of closest approach in both longitudinal and transverse directions are negligible, indicating that the effect of contaminations from secondary particles on the measurements is insignificant. Finally, tightening the χ^2 per number of TPC clusters from 4 to 2.5 gives an uncertainty of at most 3%. The total systematic uncertainty is calculated as the quadratic sum of the individual sources that have a statistically significant contribution according to a statistical test [74].

The A_2^{f} measurements as a function of the associate particle transverse momentum $p_{\mathrm{T}}^{\mathrm{a}}$ in centrality classes 0–5%, 10–20%, and 30–40% are shown in Fig. 1. The results are presented from 0.2 GeV/c up to 4 GeV/c, since the requirement of two particles at high $p_{\mathrm{T}}^{\mathrm{a}}$ for the four-particle correlations limits the available data sample at higher transverse momentum. In the most central collisions 0–5%, a large deviation from unity is observed starting from $p_{\mathrm{T}}^{\mathrm{a}} \approx 2.5$ GeV/c, which increases towards higher $p_{\mathrm{T}}^{\mathrm{a}}$ range. As previously mentioned, this deviation cannot be attributed to non-flow effects, whose contributions are negligible. With more than 5σ significance of the deviation at high $p_{\mathrm{T}}^{\mathrm{a}}$ across the presented centralities, these measurements provide the first observation of p_{T}-dependent flow angle fluctuations in Pb–Pb collisions at $\sqrt{s_{\mathrm{NN}}}$ = 5.02 TeV. In centralities 10–20% and 30–40%, the fluctuation weakens and

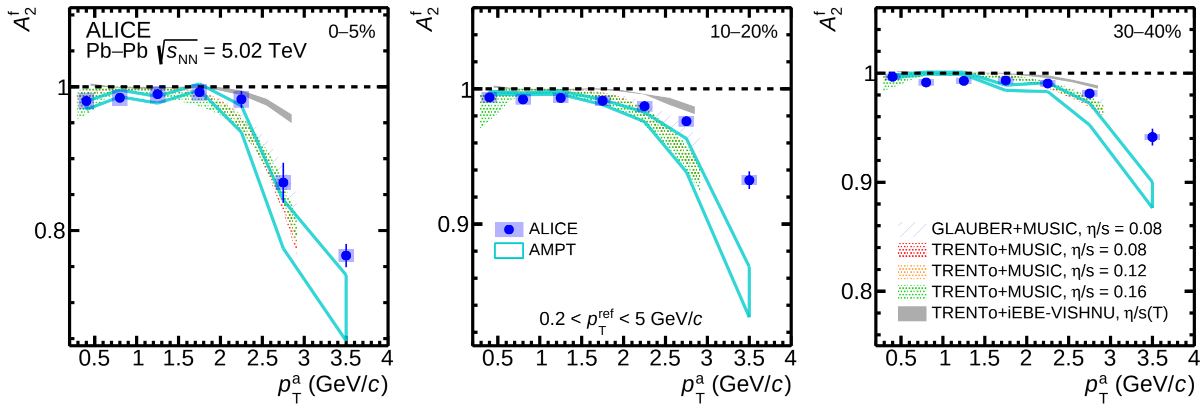

Figure 1: The flow angle fluctuation A_2^f in Pb–Pb collisions at $\sqrt{s_{NN}}$ = 5.02 TeV as a function of the associate particle transverse momentum, p_T^a, in centrality classes 0–5% (left), 10–20% (middle), and 30–40% (right). Comparison with iEBE-VISHNU with T$_R$ENTo initial conditions and $\eta/s(T)$ [76], iEBE-VISHNU with AMPT initial conditions and $\eta/s = 0.08$ [76] and $\eta/s = 0.20$, CoLBT [77], and AMPT [78] are shown as coloured bands.

reaches around 5–7% deviation from unity at high $p_T^a \approx 3.5$ GeV/c in comparison to 0–5% most central collisions. The increasing deviation from unity with p_T^a above 3 GeV/c observed in data suggests that the elliptic flow at large transverse momentum ($p_T > 2.5$ GeV/c) may not be correlated with a common symmetry plane. This will affect the comparison of measurements relying on a common symmetry plane between particles at high and low p_T with theoretical models that do not feature flow angle fluctuations, e.g. measurements of the flow of charmed hadrons, used to constrain the path-length dependence of in-medium energy loss of the heavy-quarks [53, 54] and their transport properties [75].

Theoretical calculations from iEBE-VISHNU [79], MUSIC [80, 81] as well as AMPT [78, 82] models are, when available, compared to the data in Fig. 1. The iEBE-VISHNU model is a (2+1)D viscous hydrodynamical model coupled to the hadronic cascade model UrQMD [83]. This model has been successful in describing collective phenomena in different systems and event-by-event fluctuations [76, 84]. The iEBE-VISHNU model is used with T$_R$ENTo initial conditions and has a temperature-dependent specific shear viscosity $\eta/s(T)$ [85]. The model is limited to p_T ranges below 3 GeV/c. The MUSIC model is an event-by-event (3+1D) viscous hydrodynamic model and is used with both Glauber [86] and T$_R$ENTo [87] initial conditions. Different values of the specific shear viscosity of 0.08, 0.12 and 0.16 are used with T$_R$ENTo initial conditions [88]. The AMPT transport model uses partonic interactions with string melting, and a quark coalescence model is used to simulate the formation of hadrons, which are then transported through a hadronic cascade model [89]. It is tuned to measurements of $dN/d\eta$, p_T-spectra and elliptic flow of charged pions, kaons and protons from the ALICE experiment [78, 90]. The iEBE-VISHNU calculation underestimates the deviation of A_2^f from unity at above 2.5 GeV/c across the presented centralities with the largest difference in the 0–5% most central collisions. The iEBE-VISHNU model with T$_R$ENTo initial conditions uses parameters extracted from a Bayesian analysis [85] in contrast to the MUSIC models which use standard T$_R$ENTo initial conditions [87]. The Bayesian T$_R$ENTo represents the current best understanding of the initial conditions and QGP transport properties, so these measurements bring further constraints on the state-of-the-art models. The comparison of the MUSIC calculations with Glauber and T$_R$ENTo initial conditions shows that A_2^f is sensitive to the fluctuations in the initial state with little sensitivity to the different values of specific shear viscosity. The AMPT calculation describes the data well in the 0–5% most central collisions and captures the deviation from unity in the highest p_T^a bin. At higher centralities the AMPT calculation overestimates the deviation from unity at high p_T^a.

The measurements of the p_T-dependent fluctuations of the flow magnitude, M_2^f, as a function of the transverse momentum, p_T^a, in centrality classes 0–5%, 10–20%, and 30–40% are shown in Fig. 2. A

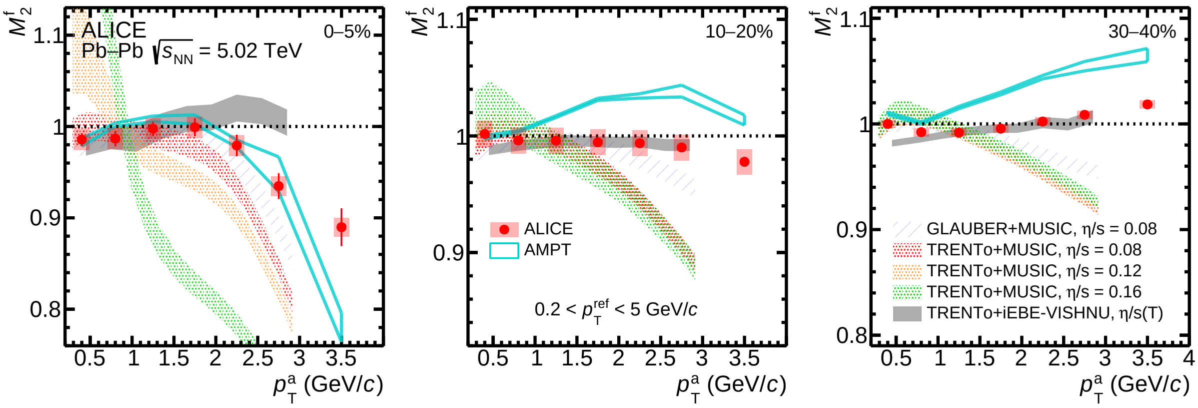

Figure 2: The flow magnitude fluctuation M_2^f in Pb–Pb collisions at $\sqrt{s_{NN}}$ = 5.02 TeV as a function of the associate particle transverse momentum, p_T^a, in centrality classes 0–5% (left), 10–20% (middle), and 30–40% (right). Comparison with iEBE-VISHNU with T$_R$ENTo initial conditions and $\eta/s(T)$ [76], MUSIC with Glauber initial conditions and $\eta/s = 0.08$ [88], MUSIC with T$_R$ENTo initial conditions and $\eta/s = 0.08, 0.12, 0.16$ [88], and AMPT [78] are shown as coloured bands.

substantial deviation of M_2^f from unity is observed in the 0–5% most central collisions. This deviation by more than 5σ significance in the highest bin of p_T^a reveals the first observation of p_T-dependent flow magnitude fluctuations in Pb–Pb collisions at $\sqrt{s_{NN}}$ = 5.02 TeV. In centrality 0–5%, where the initial state fluctuations are most significant, the flow magnitude deviates from unity for p_T^a above 2 GeV/c and the deviation increases with increasing p_T^a. The deviation from unity is more pronounced in the central collisions 0–5% compared to 10–20% and 30–40%. By construction, M_2^f is not restricted to be below unity as seen in Fig. 2 at 30–40% centrality. This is in contrast to the flow vector fluctuations measured with two-particle correlations and the flow angle fluctuations measured with A_2^f, which can only be larger than unity due to non-flow effects [56]. Model studies with HIJING and the studies of the correlators with same-sign charge and larger pseudorapidity gaps show that non-flow correlations are negligible for M_2^f, so the deviation from unity must be due to the fluctuations of the flow magnitude. The iEBE-VISHNU calculations underestimate the effect in 0–5% centrality showing almost no p_T dependence. In the 10–20% and 30–40% centrality intervals, the model captures the increasing trend with p_T^a and, consequently, describes the data. The MUSIC models show strong sensitivity to the specific shear viscosity in 0–5% most central collisions, and also a sensitivity to the different initial conditions. In the 10–20% and 30–40% centrality intervals, M_2^f shows no sensitivity to the specific shear viscosity, but is still affected by the different initial conditions. The MUSIC models overestimate the deviation of M_2^f from unity. The comparison of the measurements with these models reveals that the flow magnitude fluctuations are driven by initial state fluctuations, and that in most central collisions they are also affected by the transport properties of the QGP. The AMPT transport model calculation succeeds in describing the flow magnitude fluctuations in the most central collisions, where it also describes the flow angle fluctuations (Fig. 1 left). At higher centralities, the AMPT model significantly overestimates the data even at low p_T^a, but it qualitatively captures the increasing trend of M_2^f in the data in the 30–40% centrality interval.

In order to connect the four-particle correlation observables to the previously measured flow vector fluctuations, the limits from Eqs. (4) and (6) are compared to the flow vector fluctuations probed by Eq. (5). Thus the lower moments of the flow angle fluctuations and flow magnitude fluctuations, which cannot be directly accessed in experiments, can be explored. The lower limit on the first-order flow angle fluctuations, the upper limit on the first-order flow magnitude fluctuations, and the total flow vector fluctuations are shown as a function of centrality in the $3 < p_T^a < 4$ GeV/c range in Fig. 3. In central collisions, the upper limit on the flow magnitude fluctuations is higher than the lower limit of the flow angle fluctuations up to 10% centrality. For the 10–30% centrality interval, the limits are similar, and above 30% centrality,

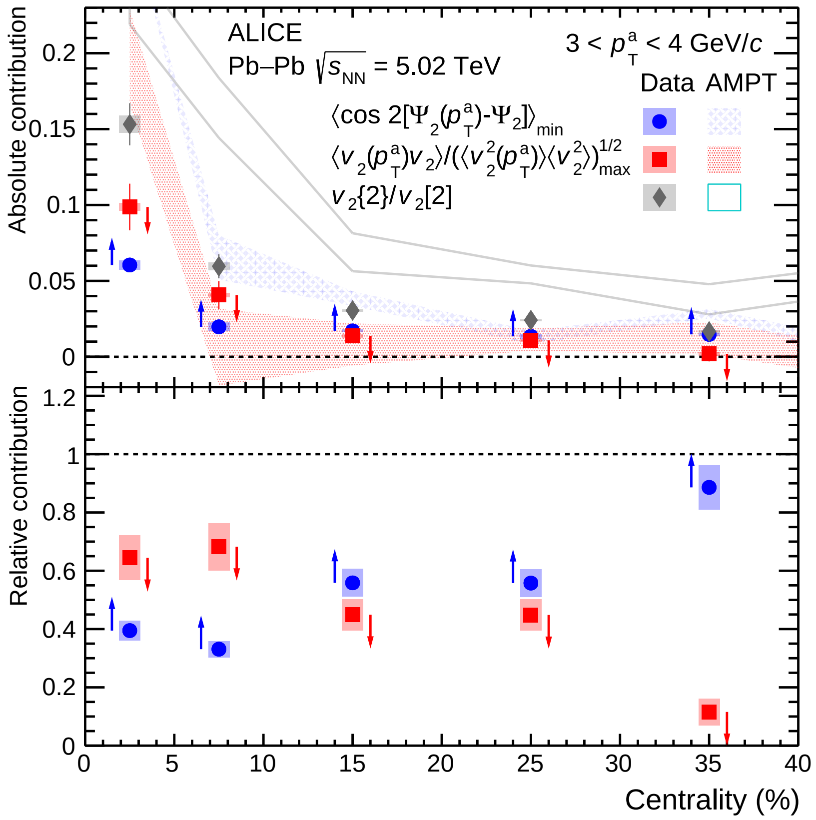

Figure 3: The lower limit of the first-order flow angle fluctuations, upper limit of the first-order flow magnitude fluctuations, and the flow vector fluctuations as a function of centrality for the $3.0 < p_T^a < 4.0$ GeV/c. The lower and upper limits are denoted by the arrows. The top panel shows the absolute contribution and the bottom panel the contribution relative to the overall flow vector fluctuations. Comparisons to AMPT [78] are shown as coloured bands.

the flow magnitude upper limits are much smaller, and the flow angle fluctuations dominate the overall flow vector fluctuations completely. This is consistent with the measurements shown in Figs. 1 and 2, where M_2^f approaches unity faster with increasing centrality than A_2^f and even goes above unity in semi-central collisions. While p_T-dependent flow angle and flow magnitude fluctuations are both present in central Pb–Pb collisions, the effects of flow angle fluctuations are consistently present across the shown centralities compared to the much smaller flow magnitude fluctuations in non-central collisions. The AMPT transport model calculations overestimate the flow vector fluctuations $v_2\{2\}/v_2[2]$ as well as the limits of the first-order flow angle and flow magnitude fluctuations in the central collisions. At higher centralities, AMPT describes the lower and upper limits well, whereas the flow vector fluctuations are still overestimated by the model as in central collisions.

In summary, the p_T-dependent flow angle fluctuations and flow magnitude fluctuations of the second-order flow vector $\vec{V}_2$ are measured in Pb–Pb collisions at $\sqrt{s_{NN}}$ = 5.02 TeV with the correlators A_2^f and M_2^f as function of the associate particle momentum in centrality intervals 0–5%, 10–20%, and 30–40%. Large deviations from unity of both A_2^f ($\sim$20%) and M_2^f ($\sim$10%) are observed in central collisions, where the event-by-event fluctuations of the position of the colliding nucleons dominate over the geometric response. In semicentral collisions, both flow angle and flow magnitude fluctuations decrease. The flow angle fluctuations reach 5–7% and the flow magnitude fluctuations reach around 2% and are above unity in 30–40% centrality. The flow magnitude fluctuations decrease faster than the flow angle fluctuations up to 40% centrality, where the flow vector fluctuations are almost solely due to flow angle fluctuations. The proposed correlators decompose the flow vector fluctuations into constituent flow angle and flow magnitude fluctuations. The observation of flow angle and flow magnitude fluctuations gives further insight into the nature of event-by-event fluctuations in the initial state of heavy-ion collisions and comparison with theoretical models provides further constraints on the initial conditions and even the QGP transport coefficient η/s in central collisions. The flow angle fluctuations and flow magnitude fluctuations are most pronounced at high p_{T} and will affect measurements that assume a common symmetry plane, such as high-p_{T} azimuthal correlations, which is the typical method for high-p_{T} flow measurements. The measurements provide further constraints on existing models, which are necessary to avoid biasing the extraction of QGP transport properties, such as the jet transport coefficient, $\hat{q}$, with flow measurements.

References

[1] E. V. Shuryak, "Quark-Gluon Plasma and Hadronic Production of Leptons, Photons and Psions", *Phys. Lett.* **B78** (1978) 150. [Yad. Fiz.28,796(1978)].

[2] E. V. Shuryak, "Quantum Chromodynamics and the Theory of Superdense Matter", *Phys. Rept.* **61** (1980) 71–158.

[3] **BRAHMS** Collaboration, I. Arsene *et al.*, "Quark gluon plasma and color glass condensate at RHIC? The Perspective from the BRAHMS experiment", *Nucl. Phys. A* **757** (2005) 1–27, `arXiv:nucl-ex/0410020`.

[4] **STAR** Collaboration, J. Adams *et al.*, "Experimental and theoretical challenges in the search for the quark gluon plasma: The STAR Collaboration's critical assessment of the evidence from RHIC collisions", *Nucl. Phys. A* **757** (2005) 102–183, `arXiv:nucl-ex/0501009`.

[5] **PHENIX** Collaboration, K. Adcox *et al.*, "Formation of dense partonic matter in relativistic nucleus-nucleus collisions at RHIC: Experimental evaluation by the PHENIX collaboration", *Nucl. Phys. A* **757** (2005) 184–283, `arXiv:nucl-ex/0410003`.

[6] **PHOBOS** Collaboration, B. B. Back *et al.*, "The PHOBOS perspective on discoveries at RHIC", *Nucl. Phys. A* **757** (2005) 28–101, `arXiv:nucl-ex/0410022`.

[7] B. Muller, J. Schukraft, and B. Wyslouch, "First Results from Pb+Pb collisions at the LHC", *Ann. Rev. Nucl. Part. Sci.* **62** (2012) 361–386, `arXiv:1202.3233 [hep-ex]`.

[8] J.-Y. Ollitrault, "Anisotropy as a signature of transverse collective flow", *Phys. Rev.* **D46** (1992) 229–245.

[9] S. A. Voloshin, A. M. Poskanzer, and R. Snellings, "Collective phenomena in non-central nuclear collisions", *Landolt-Bornstein* **23** (2010) 293–333, `arXiv:0809.2949 [nucl-ex]`.

[10] U. Heinz and R. Snellings, "Collective flow and viscosity in relativistic heavy-ion collisions", *Ann. Rev. Nucl. Part. Sci.* **63** (2013) 123–151, `arXiv:1301.2826 [nucl-th]`.

[11] S. Voloshin and Y. Zhang, "Flow study in relativistic nuclear collisions by Fourier expansion of Azimuthal particle distributions", *Z. Phys.* **C70** (1996) 665–672, `arXiv:hep-ph/9407282 [hep-ph]`.

[12] B. Alver and G. Roland, "Collision geometry fluctuations and triangular flow in heavy-ion collisions", *Phys. Rev.* **C81** (2010) 054905, `arXiv:1003.0194 [nucl-th]`. [Erratum: Phys. Rev.C82,039903(2010)].

[13] B. H. Alver, C. Gombeaud, M. Luzum, and J.-Y. Ollitrault, "Triangular flow in hydrodynamics and transport theory", *Phys. Rev.* **C82** (2010) 034913, `arXiv:1007.5469 [nucl-th]`.

[14] D. Teaney and L. Yan, "Triangularity and Dipole Asymmetry in Heavy Ion Collisions", *Phys. Rev.* **C83** (2011) 064904, arXiv:1010.1876 [nucl-th].

[15] M. Luzum, "Collective flow and long-range correlations in relativistic heavy ion collisions", *Phys. Lett.* **B696** (2011) 499–504, arXiv:1011.5773 [nucl-th].

[16] **STAR** Collaboration, K. H. Ackermann *et al.*, "Elliptic flow in Au + Au collisions at (S(NN))**(1/2) = 130 GeV", *Phys. Rev. Lett.* **86** (2001) 402–407, arXiv:nucl-ex/0009011.

[17] **PHENIX** Collaboration, S. S. Adler *et al.*, "Elliptic flow of identified hadrons in Au+Au collisions at s(NN)**(1/2) = 200-GeV", *Phys. Rev. Lett.* **91** (2003) 182301, arXiv:nucl-ex/0305013.

[18] **STAR** Collaboration, L. Adamczyk *et al.*, "Third Harmonic Flow of Charged Particles in Au+Au Collisions at sqrtsNN = 200 GeV", *Phys. Rev. C* **88** no. 1, (2013) 014904, arXiv:1301.2187 [nucl-ex].

[19] **PHENIX** Collaboration, A. Adare *et al.*, "Measurements of elliptic and triangular flow in high-multiplicity ^{3}He+Au collisions at $\sqrt{s_{_{NN}}} = 200$ GeV", *Phys. Rev. Lett.* **115** no. 14, (2015) 142301, arXiv:1507.06273 [nucl-ex].

[20] **ALICE** Collaboration, K. Aamodt *et al.*, "Elliptic flow of charged particles in Pb-Pb collisions at 2.76 TeV", *Phys. Rev. Lett.* **105** (2010) 252302, arXiv:1011.3914 [nucl-ex].

[21] **ALICE** Collaboration, K. Aamodt *et al.*, "Higher harmonic anisotropic flow measurements of charged particles in Pb-Pb collisions at $\sqrt{s_{NN}}$=2.76 TeV", *Phys. Rev. Lett.* **107** (2011) 032301, arXiv:1105.3865 [nucl-ex].

[22] **ALICE** Collaboration, B. Abelev *et al.*, "Elliptic flow of identified hadrons in Pb-Pb collisions at $\sqrt{s_{\rm NN}} = 2.76$ TeV", *JHEP* **06** (2015) 190, arXiv:1405.4632 [nucl-ex].

[23] **ALICE** Collaboration, J. Adam *et al.*, "Anisotropic flow of charged particles in Pb-Pb collisions at $\sqrt{s_{\rm NN}} = 5.02$ TeV", *Phys. Rev. Lett.* **116** no. 13, (2016) 132302, arXiv:1602.01119 [nucl-ex].

[24] **ALICE** Collaboration, S. Acharya *et al.*, "Linear and non-linear flow modes in Pb-Pb collisions at $\sqrt{s_{\rm NN}} = 2.76$ TeV", *Phys. Lett.* **B773** (2017) 68–80, arXiv:1705.04377 [nucl-ex].

[25] **ATLAS** Collaboration, G. Aad *et al.*, "Measurement of the azimuthal anisotropy for charged particle production in $\sqrt{s_{NN}} = 2.76$ TeV lead-lead collisions with the ATLAS detector", *Phys. Rev.* **C86** (2012) 014907, arXiv:1203.3087 [hep-ex].

[26] **ATLAS** Collaboration, G. Aad *et al.*, "Measurement of the pseudorapidity and transverse momentum dependence of the elliptic flow of charged particles in lead-lead collisions at $\sqrt{s_{NN}} = 2.76$ TeV with the ATLAS detector", *Phys. Lett.* **B707** (2012) 330–348, arXiv:1108.6018 [hep-ex].

[27] **ATLAS** Collaboration, G. Aad *et al.*, "Measurement of the distributions of event-by-event flow harmonics in lead-lead collisions at $\sqrt{s_{\rm NN}} = 2.76$ TeV with the ATLAS detector at the LHC", *JHEP* **11** (2013) 183, arXiv:1305.2942 [hep-ex].

[28] **CMS** Collaboration, S. Chatrchyan *et al.*, "Centrality dependence of dihadron correlations and azimuthal anisotropy harmonics in PbPb collisions at $\sqrt{s_{NN}} = 2.76$ TeV", *Eur. Phys. J.* **C72** (2012) 2012, arXiv:1201.3158 [nucl-ex].

[29] **CMS** Collaboration, S. Chatrchyan *et al.*, "Measurement of the elliptic anisotropy of charged particles produced in PbPb collisions at $\sqrt{s}_{NN}$=2.76 TeV", *Phys. Rev.* **C87** no. 1, (2013) 014902, arXiv:1204.1409 [nucl-ex].

[30] **CMS** Collaboration, S. Chatrchyan *et al.*, "Azimuthal anisotropy of charged particles at high transverse momenta in PbPb collisions at $\sqrt{s_{NN}} = 2.76$ TeV", *Phys. Rev. Lett.* **109** (2012) 022301, `arXiv:1204.1850 [nucl-ex]`.

[31] M. Luzum and H. Petersen, "Initial State Fluctuations and Final State Correlations in Relativistic Heavy-Ion Collisions", *J. Phys.* **G41** (2014) 063102, `arXiv:1312.5503 [nucl-th]`.

[32] E. Shuryak, "Strongly coupled quark-gluon plasma in heavy ion collisions", *Rev. Mod. Phys.* **89** (2017) 035001, `arXiv:1412.8393 [hep-ph]`.

[33] H. Song, Y. Zhou, and K. Gajdosova, "Collective flow and hydrodynamics in large and small systems at the LHC", *Nucl. Sci. Tech.* **28** no. 7, (2017) 99, `arXiv:1703.00670 [nucl-th]`.

[34] **PHENIX** Collaboration, A. Adare *et al.*, "Azimuthal anisotropy of neutral pion production in Au+Au collisions at $\sqrt{(s_{\rm NN})}$ = 200 GeV: Path-length dependence of jet quenching and the role of initial geometry", *Phys. Rev. Lett.* **105** (2010) 142301, `arXiv:1006.3740 [nucl-ex]`.

[35] **ALICE** Collaboration, B. Abelev *et al.*, "Anisotropic flow of charged hadrons, pions and (anti-)protons measured at high transverse momentum in Pb-Pb collisions at $\sqrt{s_{NN}}$=2.76 TeV", *Phys. Lett.* **B719** (2013) 18–28, `arXiv:1205.5761 [nucl-ex]`.

[36] **CMS** Collaboration, S. Chatrchyan *et al.*, "Azimuthal anisotropy of charged particles at high transverse momenta in PbPb collisions at $\sqrt{s_{NN}} = 2.76$ TeV", *Phys. Rev. Lett.* **109** (2012) 022301, `arXiv:1204.1850 [nucl-ex]`.

[37] **ATLAS** Collaboration, G. Aad *et al.*, "Measurement of flow harmonics with multi-particle cumulants in Pb+Pb collisions at $\sqrt{s_{\rm NN}} = 2.76$ TeV with the ATLAS detector", *Eur. Phys. J.* **C74** no. 11, (2014) 3157, `arXiv:1408.4342 [hep-ex]`.

[38] **ALICE** Collaboration, J. Adam *et al.*, "Anisotropic flow of charged particles in Pb-Pb collisions at $\sqrt{s_{\rm NN}} = 5.02$ TeV", *Phys. Rev. Lett.* **116** no. 13, (2016) 132302, `arXiv:1602.01119 [nucl-ex]`.

[39] **CMS** Collaboration, A. M. Sirunyan *et al.*, "Azimuthal anisotropy of charged particles with transverse momentum up to 100 GeV/ c in PbPb collisions at $\sqrt{s}_{NN}$=5.02 TeV", *Phys. Lett.* **B776** (2018) 195–216, `arXiv:1702.00630 [hep-ex]`.

[40] **PHENIX** Collaboration, A. Adare *et al.*, "Heavy Quark Production in $p+p$ and Energy Loss and Flow of Heavy Quarks in Au+Au Collisions at $\sqrt{s_{NN}} = 200$ GeV", *Phys. Rev.* **C84** (2011) 044905, `arXiv:1005.1627 [nucl-ex]`.

[41] **STAR** Collaboration, L. Adamczyk *et al.*, "Elliptic flow of electrons from heavy-flavor hadron decays in Au + Au collisions at $\sqrt{s_{\rm NN}} = 200$, 62.4, and 39 GeV", *Phys. Rev.* **C95** no. 3, (2017) 034907, `arXiv:1405.6348 [hep-ex]`.

[42] **STAR** Collaboration, L. Adamczyk *et al.*, "Measurement of D^0 Azimuthal Anisotropy at Midrapidity in Au+Au Collisions at $\sqrt{s_{NN}}$=200 GeV", *Phys. Rev. Lett.* **118** no. 21, (2017) 212301, `arXiv:1701.06060 [nucl-ex]`.

[43] **ALICE** Collaboration, B. Abelev *et al.*, "D meson elliptic flow in non-central Pb-Pb collisions at $\sqrt{s_{\rm NN}}$ = 2.76TeV", *Phys. Rev. Lett.* **111** (2013) 102301, `arXiv:1305.2707 [nucl-ex]`.

[44] **ALICE** Collaboration, E. Abbas *et al.*, "J/ψ Elliptic Flow in Pb–Pb Collisions at $\sqrt{s_{\rm NN}}$ = 2.76 TeV", *Phys. Rev. Lett.* **111** (2013) 162301, `arXiv:1303.5880 [nucl-ex]`.

[45] **ALICE** Collaboration, B. Abelev *et al.*, “Azimuthal anisotropy of D meson production in Pb-Pb collisions at $\sqrt{s_{\rm NN}} = 2.76$ TeV”, *Phys. Rev. C* **90** no. 3, (2014) 034904, `arXiv:1405.2001 [nucl-ex]`.

[46] **ALICE** Collaboration, J. Adam *et al.*, “Elliptic flow of electrons from heavy-flavour hadron decays at mid-rapidity in Pb-Pb collisions at $\sqrt{s_{\rm NN}} = 2.76$ TeV”, *JHEP* **09** (2016) 028, `arXiv:1606.00321 [nucl-ex]`.

[47] **ALICE** Collaboration, J. Adam *et al.*, “Elliptic flow of muons from heavy-flavour hadron decays at forward rapidity in Pb–Pb collisions at $\sqrt{s_{\rm NN}} = 2.76$ TeV”, *Phys. Lett.* **B753** (2016) 41–56, `arXiv:1507.03134 [nucl-ex]`.

[48] **ALICE** Collaboration, S. Acharya *et al.*, “*D*-meson azimuthal anisotropy in midcentral Pb-Pb collisions at $\sqrt{\mathbf{s}_{\rm NN}} = \mathbf{5.02}$ TeV”, *Phys. Rev. Lett.* **120** no. 10, (2018) 102301, `arXiv:1707.01005 [nucl-ex]`.

[49] **CMS** Collaboration, A. M. Sirunyan *et al.*, “Measurement of prompt D^0 meson azimuthal anisotropy in Pb-Pb collisions at $\sqrt{s_{\rm NN}}$ = 5.02 TeV”, *Phys. Rev. Lett.* **120** no. 20, (2018) 202301, `arXiv:1708.03497 [nucl-ex]`.

[50] **ALICE** Collaboration, S. Acharya *et al.*, “Transverse-momentum and event-shape dependence of D-meson flow harmonics in Pb–Pb collisions at $\sqrt{s_{NN}}$ = 5.02 TeV”, *Phys. Lett.* **B813** (2021) 136054, `arXiv:2005.11131 [nucl-ex]`.

[51] **ALICE** Collaboration, S. Acharya *et al.*, “Prompt D^0, D^+, and D^{*+} production in Pb–Pb collisions at $\sqrt{s_{\rm NN}}$ = 5.02 TeV”, *JHEP* **01** (2022) 174, `arXiv:2110.09420 [nucl-ex]`.

[52] **ALICE** Collaboration, S. Acharya *et al.*, “Measurement of prompt D_s^+-meson production and azimuthal anisotropy in Pb–Pb collisions at $\sqrt{s_{NN}}$=5.02TeV”, *Phys. Lett.* **B827** (2022) 136986, `arXiv:2110.10006 [nucl-ex]`.

[53] M. Gyulassy, I. Vitev, and X. N. Wang, “High p(T) azimuthal asymmetry in noncentral A+A at RHIC”, *Phys. Rev. Lett.* **86** (2001) 2537–2540, `arXiv:nucl-th/0012092`.

[54] E. V. Shuryak, “The Azimuthal asymmetry at large p(t) seem to be too large for a ‘jet quenching’”, *Phys. Rev.* **C66** (2002) 027902, `arXiv:nucl-th/0112042`.

[55] U. Heinz, Z. Qiu, and C. Shen, “Fluctuating flow angles and anisotropic flow measurements”, *Phys. Rev.* **C87** no. 3, (2013) 034913, `arXiv:1302.3535 [nucl-th]`.

[56] F. G. Gardim, F. Grassi, M. Luzum, and J.-Y. Ollitrault, “Breaking of factorization of two-particle correlations in hydrodynamics”, *Phys. Rev.* **C87** no. 3, (2013) 031901, `arXiv:1211.0989 [nucl-th]`.

[57] **ALICE** Collaboration, S. Acharya *et al.*, “Searches for transverse momentum dependent flow vector fluctuations in Pb-Pb and p-Pb collisions at the LHC”, *JHEP* **09** (2017) 032, `arXiv:1707.05690 [nucl-ex]`.

[58] **CMS** Collaboration, S. Chatrchyan *et al.*, “Studies of azimuthal dihadron correlations in ultra-central PbPb collisions at $\sqrt{s_{NN}} = 2.76$ TeV”, *JHEP* **02** (2014) 088, `arXiv:1312.1845 [nucl-ex]`.

[59] **CMS** Collaboration, V. Khachatryan *et al.*, “Evidence for transverse momentum and pseudorapidity dependent event plane fluctuations in PbPb and pPb collisions”, *Phys. Rev.* **C92** no. 3, (2015) 034911, `arXiv:1503.01692 [nucl-ex]`.

[60] **ALICE** Collaboration, K. Aamodt *et al.*, "Harmonic decomposition of two-particle angular correlations in Pb-Pb collisions at $\sqrt{s_{\rm NN}} = 2.76$ TeV", *Phys. Lett.* **B708** (2012) 249–264, arXiv:1109.2501 [nucl-ex].

[61] R. S. Bhalerao, J.-Y. Ollitrault, S. Pal, and D. Teaney, "Principal component analysis of event-by-event fluctuations", *Phys. Rev. Lett.* **114** no. 15, (2015) 152301, arXiv:1410.7739 [nucl-th].

[62] Z. Liu, W. Zhao, and H. Song, "Principal Component Analysis of collective flow in Relativistic Heavy-Ion Collisions", *Eur. Phys. J.* **C79** no. 10, (2019) 870, arXiv:1903.09833 [nucl-th].

[63] Z. Liu, A. Behera, H. Song, and J. Jia, "Robustness of principal component analysis of harmonic flow in heavy ion collisions", *Phys. Rev.* **C102** no. 2, (2020) 024911, arXiv:2002.06061 [nucl-ex].

[64] M. Hippert, D. Dobrigkeit Chinellato, M. Luzum, J. Noronha, T. Nunes da Silva, and J. Takahashi, "Measuring Momentum-Dependent Flow Fluctuations in Heavy-Ion Collisions", *Phys. Rev.* **C101** no. 3, (2020) 034903, arXiv:1906.08915 [nucl-th].

[65] P. Bozek and W. Broniowski, "Longitudinal decorrelation measures of flow magnitude and event-plane angles in ultrarelativistic nuclear collisions", *Phys. Rev. C* **97** no. 3, (2018) 034913, arXiv:1711.03325 [nucl-th].

[66] A. Bilandzic, C. H. Christensen, K. Gulbrandsen, A. Hansen, and Y. Zhou, "Generic framework for anisotropic flow analyses with multiparticle azimuthal correlations", *Phys. Rev.* **C89** no. 6, (2014) 064904, arXiv:1312.3572 [nucl-ex].

[67] Z. Moravcova, K. Gulbrandsen, and Y. Zhou, "Generic algorithm for multiparticle cumulants of azimuthal correlations in high energy nucleus collisions", *Phys. Rev.* **C103** no. 2, (2021) 024913, arXiv:2005.07974 [nucl-th].

[68] **ALICE** Collaboration, B. Abelev *et al.*, "Performance of the ALICE Experiment at the CERN LHC", *Int. J. Mod. Phys.* **A29** (2014) 1430044, arXiv:1402.4476 [nucl-ex].

[69] **ALICE** Collaboration, B. Abelev *et al.*, "Centrality determination of Pb-Pb collisions at $\sqrt{s_{NN}} =$ 2.76 TeV with ALICE", *Phys. Rev.* **C88** no. 4, (2013) 044909, arXiv:1301.4361 [nucl-ex].

[70] **ALICE** Collaboration, K. Aamodt *et al.*, "Alignment of the ALICE Inner Tracking System with cosmic-ray tracks", *JINST* **5** (2010) P03003, arXiv:1001.0502 [physics.ins-det].

[71] J. Alme *et al.*, "The ALICE TPC, a large 3-dimensional tracking device with fast readout for ultra-high multiplicity events", *Nucl. Instrum. Meth.* **A622** (2010) 316–367, arXiv:1001.1950 [physics.ins-det].

[72] **ALICE** Collaboration, "The ALICE definition of primary particles", *ALICE-PUBLIC-2017-005* (Jun, 2017) . https://cds.cern.ch/record/2270008.

[73] X.-N. Wang and M. Gyulassy, "hijing: A monte carlo model for multiple jet production in pp, pA, and AA collisions", *Phys. Rev.* **D44** (Dec, 1991) 3501–3516.

[74] R. Barlow, "Systematic errors: Facts and fictions", in *Conference on Advanced Statistical Techniques in Particle Physics*, pp. 134–144. 7, 2002. arXiv:hep-ex/0207026.

[75] W. Ke, Y. Xu, and S. A. Bass, "Linearized Boltzmann-Langevin model for heavy quark transport in hot and dense QCD matter", *Phys. Rev.* **C98** no. 6, (2018) 064901, arXiv:1806.08848 [nucl-th].

[76] W. Zhao, H.-j. Xu, and H. Song, "Collective flow in 2.76 A TeV and 5.02 A TeV Pb+Pb collisions", *Eur. Phys. J.* **C77** no. 9, (2017) 645, arXiv:1703.10792 [nucl-th].

[77] W. Zhao, W. Ke, W. Chen, T. Luo, and X.-N. Wang, "From Hydrodynamics to Jet Quenching, Coalescence, and Hadron Cascade: A Coupled Approach to Solving the RAA⊗v2 Puzzle", *Phys. Rev. Lett.* **128** no. 2, (2022) 022302, arXiv:2103.14657 [hep-ph].

[78] G.-L. Ma and Z.-W. Lin, "Predictions for $\sqrt{s_{NN}} = 5.02$ TeV Pb+Pb Collisions from a Multi-Phase Transport Model", *Phys. Rev.* **C93** no. 5, (2016) 054911, arXiv:1601.08160 [nucl-th].

[79] C. Shen, Z. Qiu, H. Song, J. Bernhard, S. Bass, and U. Heinz, "The iEBE-VISHNU code package for relativistic heavy-ion collisions", *Comput. Phys. Commun.* **199** (2016) 61–85, arXiv:1409.8164 [nucl-th].

[80] B. Schenke, S. Jeon, and C. Gale, "Elliptic and triangular flow in event-by-event (3+1)D viscous hydrodynamics", *Phys. Rev. Lett.* **106** (2011) 042301, arXiv:1009.3244 [hep-ph].

[81] B. Schenke, S. Jeon, and C. Gale, "(3+1)D hydrodynamic simulation of relativistic heavy-ion collisions", *Phys. Rev.* **C82** (2010) 014903, arXiv:1004.1408 [hep-ph].

[82] Z.-W. Lin, C. M. Ko, B.-A. Li, B. Zhang, and S. Pal, "A Multi-phase transport model for relativistic heavy ion collisions", *Phys. Rev.* **C72** (2005) 064901, arXiv:nucl-th/0411110 [nucl-th].

[83] S. A. Bass *et al.*, "Microscopic models for ultrarelativistic heavy ion collisions", *Prog. Part. Nucl. Phys.* **41** (1998) 255–369, arXiv:nucl-th/9803035 [nucl-th].

[84] M. Li, Y. Zhou, W. Zhao, B. Fu, Y. Mou, and H. Song, "Investigations on mixed harmonic cumulants in heavy-ion collisions at energies available at the CERN Large Hadron Collider", *Phys. Rev.* **C104** no. 2, (2021) 024903, arXiv:2104.10422 [nucl-th].

[85] J. E. Bernhard, J. S. Moreland, S. A. Bass, J. Liu, and U. Heinz, "Applying Bayesian parameter estimation to relativistic heavy-ion collisions: simultaneous characterization of the initial state and quark-gluon plasma medium", *Phys. Rev.* **C94** no. 2, (2016) 024907, arXiv:1605.03954 [nucl-th].

[86] P. Bożek, W. Broniowski, M. Rybczynski, and G. Stefanek, "GLISSANDO 3: GLauber Initial-State Simulation AND mOre..., ver. 3", *Comput. Phys. Commun.* **245** (2019) 106850, arXiv:1901.04484 [nucl-th].

[87] J. S. Moreland, J. E. Bernhard, and S. A. Bass, "Alternative ansatz to wounded nucleon and binary collision scaling in high-energy nuclear collisions", *Phys. Rev.* **C92** no. 1, (2015) 011901, arXiv:1412.4708 [nucl-th].

[88] P. Bozek and R. Samanta, "Factorization breaking for higher moments of harmonic flow", arXiv:2109.07781 [nucl-th].

[89] B.-A. Li and C. M. Ko, "Formation of superdense hadronic matter in high-energy heavy ion collisions", *Phys. Rev.* **C52** (1995) 2037–2063, arXiv:nucl-th/9505016 [nucl-th].

[90] J. Xu and C. M. Ko, "Pb-Pb collisions at $\sqrt{s_{NN}} = 2.76$ TeV in a multiphase transport model", *Phys. Rev. C* **83** (2011) 034904, arXiv:1101.2231 [nucl-th].